Degrees of Freedom in Scattered Fields for Trade-off in Joint Communications and Sensing

Husheng Li

***Abstract*—In joint communications and sensing (JCS), the same electromagnetic (EM) wave is used for both functions, in the forward (incident) and backward (scattered) channels, respectively. The communication channel is determined by scatterers (also as sensing targets), thus coupling the performances of communications and sensing. More scattering targets generate more degrees of freedom (DoFs) for communications, thus improving the channel capacity given sufficient antennas. Meanwhile, they also result in more sensing errors due to the increasing complexity of EM field. The complexity analysis of EM field, in terms of DoFs, is applied to analyze the trade-off between communications and sensing, as the complexity of scattering targets increases. Numerical results are calculated to demonstrate the performance trade-off between communications and sensing.**

I. Introduction

The technology of joint communications and sensing (JCS) has received substantial attentions in recent years, due to its expected improvement of spectral and power efficiencies [1]–[5]. As illustrated in Fig. 1, a JCS transceiver sends an electromagnetic (EM) wave, which is modulated by communication data. When there is no significant scatterer or obstacle, the EM wave arrives directly at a communication receiver and thus delivers the information. No detection of scattered EM wave at the JCS transceiver (which is also equipped with receive antennas) implies the nonexistence of scattering targets. When there are significant scatterers, the incident EM wave is scattered; a portion of the scattered wave (possibly in addition to the line-of-sight (LOS) wave) is received by the communication receiver, thus accomplishing the task of communications. Meanwhile another portion of the scattered wave is received by the JCS transceiver, from which the information of scatterers (such as distance, velocity and reflectivity) can be inferred, thus completing the task of radar sensing. Since the same waveform is used for both functions, the spectrum bandwidth is substantially saved, which benefits the development of cyber physical systems (CPSs) that need communications and sensing simultaneously.

A major concern in JCS is the interdependency between communications and sensing. In particular, it is critical to identify their conflict of interests, from various viewpoints such as the different power spectral densities (PSDs) (studied by the author in [6]) and the waveform uncertainty (studied by the author in [7]). In this paper, we focus on the performance conflict due to the complexity of the scatterers, assuming that both the JCS transceiver and communication receiver are equipped with antenna arrays. On one hand, more scatterers tend to generate a higher rank for the communication channel matrix, which benefits communications; on the other hand, more scatterers, as radar sensing targets, make the received signal at the JCS transceiver more complex, thus increasing the mean square error (MSE) of sensing.

H. Li is with the Department of Electrical Engineering and Computer Science, the University of Tennessee, Knoxville, TN (email: husheng@eecs.utk.edu, phone number: 865-974-3861, address: 312 Min Kao Building, 1520 Middle Drive, Knoxville, TN, 37996).

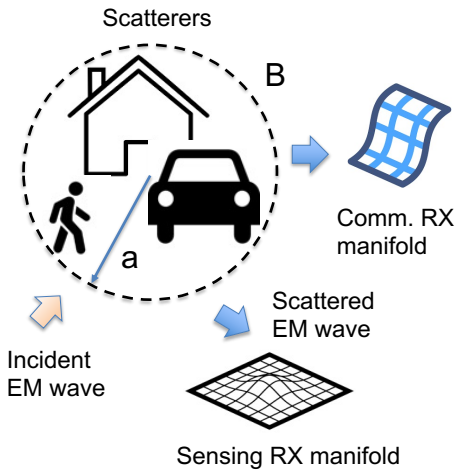

Fig. 1. System setup: scatters and receiving manifolds.

To study the complexity of the EM field generated by scatterers, we adopt the framework of degrees of freedom (DoFs) for harmonic EM field subject to scatterings [8], [9]. The DoF of EM field essentially describes the complexity that the EM field could result in over a given manifold, in terms of image reconstruction errors using a set of functions with limited spatial bandwidth. The higher the DoF is, the more information the communication could deliver through more independent channels, while more sensing errors could be incurred due to the limited number of antennas at the JCS transceiver. Existing studies have shown that the DoF of EM field is dependent on the spatial radius of the scatterers [8], [9]. Therefore, we can leverage the existing theory of EM field DoF, with substantial modifications for the context of JCS, to study the trade-off between communications and sensing due to the complexity of the environmental scattering. To our best knowledge, this is the first study on the conflict between communications and sensing in JCS from the viewpoint of EM field DoF.

The remainder of the paper is organized as follows. The related work, including the state-of-the-art of JCS and the theory of EM field DoF, is introduced in Section II. The system model and problem formulation are given in Section III. The EM field DoF and the performance trade-off are analyzed in Sections IV and V, respectively. Numerical results are provided in Section VI, while conclusions are given in Section VII.

II. Related Work

In this section, we introduce related studies.

A. JCS: State-of-the-Art

Comprehensive surveys for the JCS technology can be found in [1]–[5]. There have not been many studied on the theoretical aspect of JCS. In [10], information theoretic analysis is carried out similarly to the rate-distortion theory. An EM field analysis for JCS has been carried by the author in [11], which uses the eigen-decomposition of EM fields, instead of the DoF of fields. Most studies have been focused on the JCS algorithms, in particular the co-existence of communication and sensing, such as the spatial separation via beamforming [2], [4], [5] the time/frequency separation [12], [13], as well as nonlinear and inseparable integration [14], [15].

B. DoF of EM Field

We briefly introduce the theory of DoF in scattered EM field [8], [9]. Consider an EM field of wavenumber β, with a set of scatterers all within a ball B of radius α. The scattered field $\mathbf{E}$ is measured over a manifold $\mathcal{M}$. The DoF of the scattered field means the complexity of the possible EM fields over the manifold $\mathcal{M}$. Denote by $\mathcal{B}_w$ the set of functions on $\mathcal{M}$ with spatial bandwidth w. Then, we consider the error of using the functions in $\mathcal{B}_w$ to represent the field over $\mathcal{M}$:

$$\delta_w = \sup_{\mathbf{E}} \inf_{\mathbf{B}\in\mathcal{B}_w} \|\mathbf{E}-\mathbf{B}\|, \tag{1}$$

namely the maximum error for the representation using $\mathcal{B}_w$. The major conclusions in [8] consist of

- There exists a critical bandwidth $W_0 \approx \alpha\beta$.
- For $w < W_0$, $\delta_w \approx 1$.
- For $w > W_0$, δ_w is very small, namely

$$\delta_w \approx \frac{\exp\left(-\frac{2}{3}\sigma^{\frac{2}{3}}\right)}{\sqrt{2\pi\sigma^{\frac{3}{2}}}}, \text{ where } \sigma \approx \frac{w-W_0}{W_0^{\frac{1}{3}}}. \tag{2}$$

The DoF analysis of EM field is then applied to multi-input-multi-output (MIMO) communications [16]. Then, the relation between the DoF theory of EM field and information theory is identified in [17]. The conclusions are used to analyze the capacity of wireless networks in [18], which results in a physics-based scaling law of data throughput. However, it has not been applied in the context of JCS.

III. System Model

For simplicity of analysis, we omit the impact of noise by assuming high signal-to-noise ratio (SNR), thus focusing on the impact of DoF. Different from the setup in the theory of EM field DoF, it is assumed that a set of scatterers within N disjoint balls $\{B_n\}_{n=1,\dots,N}$ of radius $\{\alpha_n\}_{n=1,\dots,N}$. This change of setup is more suitable for the context of JCS, since the significant targets of sensing are usually sparse. Therefore, the purpose of sensing is to sense or image the significant targets (as scatterers). Moreover, the targets could be widely dispersed, thus making the radius α in the DoF analysis very large and meaningless. We further assume that all the N balls are within a ball B with radius α. The center of B is defined as the origin of the coordinate system.

We consider two receiver manifolds $\mathcal{M}_c$ and $\mathcal{M}_s$ in Fig. 1, corresponding to communication and sensing, respectively. We ignore the details of the incident EM wave emitted by the JCS transmitter and thus consider only the scattered waves. The field at position $\mathbf{r}$ is given by

$$E(\mathbf{r}) = \sum_{n=1}^{N} \int_{B_n} G(\mathbf{r},\mathbf{r}')J(\mathbf{r}')d\mathbf{r}', \tag{3}$$

where J is the source current density at the scatterers and G is the Green function of EM field, which is given by [8], [9]

$$G(\mathbf{r},\mathbf{r}') = \frac{-j\omega\mu}{4\pi R}\exp(j\beta(r-R)), \tag{4}$$

where ω is the radian frequency, μ is the magnetic permeability, $R = \|\mathbf{r}-\mathbf{r}'\|$ is the distance, $r = \|\mathbf{r}\|$ and β is the wavenumber. Notice that, compared with traditional Green function $G(\mathbf{r},\mathbf{r}') = \frac{-j\omega\mu}{4\pi R}\exp(-j\beta R)$, there is an extra term $\exp(j\beta r)$ in (4). The purpose is to compensate the factor $\exp(-j\beta R)$ when $R \to \infty$, which makes the subsequent analysis convenient.

We assume that N_s and N_c antennas are used at the receivers of sensing and communications, respectively. The corresponding spatial densities of antennas (in terms of antenna number per square meter) are denoted by ρ_s and ρ_c, respectively.

IV. EM Field DoF Analysis

In this section, we analyze the DoF of the EM field with JCS, based on which we obtain bounds for the sensing error.

A. Spatial Bandwidth

We focus on the sensing manifold $\mathcal{M}_s$ and assume that $\mathcal{M}_s$ is one-dimensional for the simplicity of analysis, without loss of generality. As shown in [8], the extension to practical 2- or 3-dimension manifolds is straightforward. Similarly to the analysis in [8], we consider the set of signals $\mathcal{B}_w$ of spatial bandwidth w. Each point $\mathbf{r}$ is parameterized by the curve length s normalized by the minimal distance from the origin to $\mathcal{M}_s$ (denoted by r_m). The EM field on $\mathcal{M}_s$ is then denoted by $E(s)$. Since the spatial bandwidth of $\mathcal{B}_s$ is limited, the estimated field needs to be projected into $\mathcal{B}_w$, thus resulting in the spatial-spectrum-truncated measurements:

$$E_w = \frac{w}{\pi}\text{sinc}(ws) * E(s), \tag{5}$$

where the sinc function is defined as $\sin(x)/x$ and stems from the Fourier transform of the rectangular function, and $*$ is convolution. Therefore, the projected field estimation E_w is given by

$$E_w(s) = \sum_{n=1}^{N} \int_{B_n} \bar{G}(s,\mathbf{r}')J(\mathbf{r}')d\mathbf{r}', \tag{6}$$

where the modified Green function is given by

$$\bar{G}(s,\mathbf{r}') = \frac{w}{\pi}\text{sinc}(ws) * G(\mathbf{s},\mathbf{r}'). \tag{7}$$

Hence, the measurement error $\Delta E(s) = E_w(s) - E(s)$ can be written as the following convolution form:

$$\Delta E(s) = \sum_{n=1}^{N} \int_{B_n} \Delta G(s,\mathbf{r}')J(\mathbf{r}')d\mathbf{r}', \tag{8}$$

where $\Delta G = G_w - G$ is the error Green function. It is given by (ref. Eq. (16) in [8])

$$\begin{aligned}\Delta G &= -\frac{\omega\mu}{8\pi^2}\int_{C^+}\frac{\exp\left(j\psi(\xi,\mathbf{r}')+jw(\xi-s)\right))}{(\xi-s)R(\xi,\mathbf{r}')}d\xi \\ &+ \frac{\omega\mu}{8\pi^2}\int_{C^-}\frac{\exp\left(j\psi(\xi,\mathbf{r}')-jw(\xi-s)\right))}{(\xi-s)R(\xi,\mathbf{r}')}d\xi, \quad (9)\end{aligned}$$

where C^+ is the path of increasing s and C^- is the opposite, and the phase factor ψ in the Green function is given by

$$\psi(s,\mathbf{r}') = \beta(r(s) - R(s,\mathbf{r}')). \quad (10)$$

According to the Cauchy-Schwartz inequality, we have

$$\|\Delta E\|_2 \le \sum_{n=1}^{N} P_n \max_{\mathbf{r}'\in B_n}\left(\int_{-\infty}^{\infty}|\Delta G(s,\mathbf{r}')|^2 ds\right)^{\frac{1}{2}} \quad (11)$$

where $P_n = \left(\int_{B_n}|J(\mathbf{r})|^2 d\mathbf{r}'\right)^{\frac{1}{2}}$ is the root mean square (RMS) of the current density in the n-th ball. Then the challenge is how to bound the integral of ΔG.

Suppose that $\beta\alpha_n$ is large for every n, namely the size of each scatter is of a higher magnitude of order than the wavelength, which is obviously true for typical wireless communications (e.g., the wavelength is 5mm for 60GHz millimeter wave). Therefore, the maximum of the integral $\int_{-\infty}^{\infty}|\Delta G(s,\mathbf{r}')|^2 ds$ can be obtained from the Laplace method [19]. To this end, we compute the stationary points for the phase factor $j\psi(\xi,\mathbf{r}') \pm jw(\xi - s))$ in (9), which is given by

$$\pm w + \frac{d}{d\xi}\psi(\xi,\mathbf{r}') = \pm w + \beta\frac{d}{d\xi}(r(\xi) - R(\xi,\mathbf{r}')) = 0. \quad (12)$$

We define the spatial bandwidth w_0, which is a function of $\mathbf{r}'$:

$$w_0 = \max_{\xi}\left|\frac{d}{d\xi}\psi(\xi,\mathbf{r}')\right|. \quad (13)$$

Then, when $w > w_0$, ΔG drops quickly as w increases; while ΔG is large when $w < w_0$, which implies large measurement errors. Therefore, the signal spacial bandwidth w is required to be less than the critical bandwidth w_0. Following the same derivation in [8] for each n, we obtain the upper bound for the error $\|\Delta E\|_2$:

$$\|\Delta E\|_2 \le \frac{\omega\mu}{4\pi d}\sum_{n=1}^{N}\left|\int_B |J(\mathbf{r}')|^2 d\mathbf{r}'\right|^{\frac{1}{2}}\frac{\exp\left(-\frac{2}{3}\sigma_{m,n}^{\frac{3}{2}}\right)}{2(w - W_n)}, \quad (14)$$

where $W_n = \max_{\mathbf{r}'\in B_n} w_0(\mathbf{r}')$, $d = \min_{s,\mathbf{r}'} R(s,\mathbf{r}')$ and

$$\sigma_{m,n} = \min_{\mathbf{r}'\in B_n}\left(\frac{2}{\dddot{\psi}(\xi_0)}\right)^{\frac{1}{3}}(w - w_0(\mathbf{r}')), \quad (15)$$

where the function ψ is defined in (10), $\dddot{\psi}$ is the third order derivative of ψ, and ξ_0 is the solution to (12).

For small errors in (14), we require $w \ge W$, where $W = \max_n W_n$. Therefore, a major challenge is how to calculate W_n for each n. Note that in [19], W is calculated for a single ball B. For the case of multiple balls of scatters in this paper, we need modifications in the analysis. To this end, we evaluate the derivative of ψ (dependent on $\mathbf{r}'$) in B_n in (13), which is given by

$$\dot{\psi}_n = \beta r_n(\hat{\mathbf{r}} - \hat{\mathbf{R}})\cdot\hat{\mathbf{v}}, \quad (16)$$

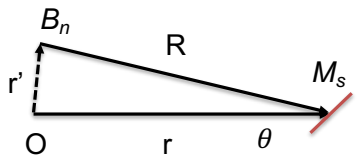

Fig. 2. Geometry for deriving (17).

where r_n is the closest distance from the ball B_n to $\mathcal{M}_s$, $\hat{\mathbf{r}}$ and $\hat{\mathbf{R}}$ are the unit direction vectors of $\mathbf{r}$ and $\mathbf{R}$, respectively, and $\hat{\mathbf{v}}$ is the unit vector of tangent at $\mathbf{r}'$.

For simplicity, we assume that $\mathcal{M}_s$ is a straight line, which is reasonable for linear antenna arrays. The corresponding equation is given by $\mathbf{r} = \mathbf{r}_0 + \mathbf{v}t$, where t is the arc length parameter and $\xi = r_m t$. Moreover, we consider only the center of B_n, denoted by $\mathbf{r}'_n$, by assuming that B_n is sufficiently small. We further assume the far field case, namely $\|\mathbf{r}\|$ and $\|\mathbf{R}\|$ are much greater than the size of $\mathcal{M}_s$. Then, we have the following approximation based on (16) and the geometry in Fig. 2:

$$\dot{\psi}_n \approx \beta r_m \sin\theta\hat{\mathbf{r}}'_n\cdot\hat{\mathbf{v}} \approx \beta\mathbf{r}'_n\cdot\hat{\mathbf{v}} \le \beta\alpha. \quad (17)$$

Therefore we have

$$W = \max_n \beta\mathbf{r}'_n\cdot\hat{\mathbf{v}} \le \beta\alpha. \quad (18)$$

B. Field Measurement Error

Given the spatial bandwidth analysis, we obtain the following proposition for an upper bound of the field measurement error, which is incurred by the limited bandwidth of function representation.

Proposition 1. *Given the above system setup and definitions, the 2-norm of the field measurement error over $\mathcal{M}_s$ is upper bounded by*

$$\|\Delta E\|_2 \le \frac{\omega\mu}{4\pi d}\sum_{n=1}^{N}\left|\int_B |J(\mathbf{r}')|^2 d\mathbf{r}'\right|^{\frac{1}{2}}\frac{\exp\left(-\frac{2}{3}\sigma_{m,n}^{\frac{3}{2}}\right)}{2(w - W)}, \quad (19)$$

C. Source Estimation Error

Now, we analyze the sensing error, namely the error of estimating the source current densities J at the scatterers, based on the measurement error analysis. For simplicity, we assume that all scatters are located within a ball B ($N = 1$).

1) Finite Expansion: For simplicity, we consider a single scatterer within a ball B. The analysis follows the following argument. If a current density $J_0(\mathbf{r}')$, $\mathbf{r}' \in B$, results in

$$\int_B G(\mathbf{r},\mathbf{r}')J_0(\mathbf{r}')d\mathbf{r}' = 0, \qquad \forall\mathbf{r}\in\mathcal{M}_s, \quad (20)$$

namely the current density J_0 generates a zero field over the sensing manifold $\mathcal{M}_s$, then the estimation error could be an arbitrary multiple of J_0, since

$$\int_B G(\mathbf{r},\mathbf{r}')(J_0(\mathbf{r}') + J(\mathbf{r}'))d\mathbf{r}' = \int_B G(\mathbf{r},\mathbf{r}')J(\mathbf{r}')d\mathbf{r}', \quad (21)$$

namely the radar sensing cannot distinguish $J_0 + J$ and J using the limited measurement over $\mathcal{M}_s$. Therefore, the worst estimation error could be arbitrarily large.

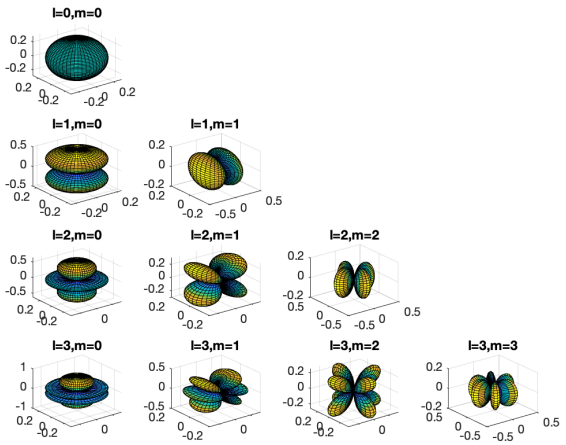

Fig. 3. Examples of spherical harmonic functions.

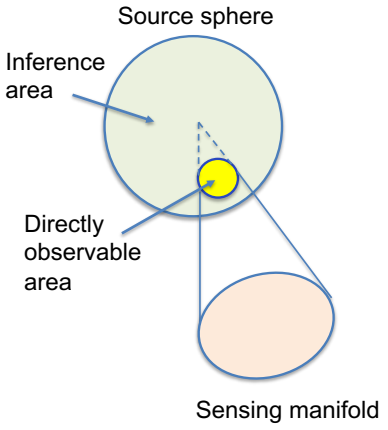

Fig. 4. Observable region and sensing manifold.

To bound the estimation error, we need the following two stages of analysis: (1) Decompose the Green function into patterns, namely carrying out an eigen decomposition. (2) Limit the source J to a subset of the patterns, thus making (20) impossible.

To this end, we consider the following spherical decomposition of Green function [20]:

$$G(\mathbf{r},\mathbf{r}') = -jk\sum_{l=0}^{\infty}\sum_{m=-l}^{l} j_l(kr_<)h_l^+(kr_>)Y_l^m(\hat{\mathbf{r}})Y_l^{m*}(\hat{\mathbf{r}}'), \quad (22)$$

where the notation is as follows:

- $k = \frac{2\pi}{\lambda}$ is the wavenumber. $r = |\mathbf{r}|$, $\hat{\mathbf{r}} = \frac{\mathbf{r}}{r}$, $r_< = \min\{r, r'\}$, $r_> = \max\{r, r'\}$.
- j_l is the l-th order spherical Bessel function given by $j_l(kr) = \sqrt{\frac{\pi}{2kr}}J_{l+\frac{1}{2}}(kr)$, where $J_{l+\frac{1}{2}}$ is the ordinary Bessel function.
- h_l is the spherical Hankel function and is defined as $h_l(z) = j_l(z) + jn_l(z)$, where $n_l(z)$ is the spherical Neumann function and is defined as $n_l(kr) = \sqrt{\frac{\pi}{2kr}}N_{l+\frac{1}{2}}(kr)$ (N is the ordinary Neumann function).
- Y_l^m is the spherical harmonics function, defined as

$$\begin{aligned} & Y_l^m(\theta,\phi) \\ = \; & (-1)^m\sqrt{\frac{2l+1}{4\pi}\frac{(l-m)!}{(l+m)!}}P_l^m(\cos\theta)e^{km\phi}, \quad (23) \end{aligned}$$

  where P_l^m is the Legendre polynomial. Examples of the spherical harmonic functions are shown in Fig. 3, with $l = 0, ..., 3$ and $0 \le m \le l$. We observe that the spacial pattern becomes more complex when l increases.

For simplicity of analysis and without loss of generality, we assume that $\mathcal{M}_s$ is a portion of spherical surface with constant distance r to the origin. Moreover, we assume that directional angle of $\mathcal{M}_s$ is within $[\theta_1, \theta_2] \times [\phi_1, \phi_2]$. We can rewrite the Green function $G(\mathbf{r}, \mathbf{r}')$ as

$$\begin{aligned} G(\mathbf{r},\mathbf{r}') &= G(\theta,\phi,r',\theta',\phi') \\ &\propto \sum_{l=0}^{\infty}\sum_{m=-l}^{l} j_l(r')Y_l^m(\theta,\phi)Y_l^{m*}(\theta',\phi'), \quad (24) \end{aligned}$$

where (r', θ', ϕ') is the polar coordinates of $\mathbf{r}'$.

Due to the completeness of the family of spherical harmonics, the current density $J(\mathbf{r}')$ can also be expanded as the series of spherical harmonics. As mentioned above, higher order spherical harmonics mean more rapid change in the space. Due to the smoothness of targets, it is reasonable to assume that the order of spherical harmonics in J is limited to L with negligible residual errors, where L can be determined using experiments. Moreover, we assume that the currents are located on the sphere surface. Hence, the current density can be written as

$$J(\mathbf{r}') = \sum_{l=0}^{L}\sum_{m=-l}^{l} c_l^m Y_l^m(\theta',\phi'), \quad (25)$$

where c_l^m is the coefficient of the (l, m)-harmonics.

Since the spherical harmonics function is orthogonal, namely (Eq. (3.31) in [20])

$$\int_B Y_l^m(\theta,\phi)Y_{l'}^{m'*}(\theta,\phi)d\theta d\phi = \delta_{l,l'}\delta_{m,m'}, \quad (26)$$

the integral in (3) is then simplified to

$$\begin{aligned} E(\mathbf{r}) &= \sum_{l=0}^{\infty}\sum_{m=-l}^{l} j_l(r')Y_l^m(\theta,\phi) \\ &\times \sum_{l'=0}^{\infty}\sum_{m'=-l'}^{l'} c_l^m\int_B Y_l^{m*}(\theta',\phi')Y_{l'}^{m'}(\theta',\phi')d\theta' d\phi' \\ &= j_l(r')\sum_{l=0}^{L}\sum_{m=-l}^{l} c_l^m Y_l^m(\theta,\phi) = j_l(r')J(\mathbf{r}). \quad (27) \end{aligned}$$

An interesting observation is that the field $E(\mathbf{r})$ is proportional to the current density at the same direction, as illustrated in Fig. 4. When L is infinite, we can only estimation the current densities within the same angle range of the sensing manifold, thus leaving unbounded errors beyond this range. Thanks to the assumption of finitely many modes of spherical harmonics in the source current density, we can use the observations $E(\mathbf{r})$, $\mathbf{r} \in \mathcal{M}_s$, to estimate the finite dimensional mode coefficients $\{c_m^l\}_{l=0,...,L,m=-l,...,l}$ and interpolate the directly observable $J(\mathbf{r}')$ over $\mathcal{M}_s$ to the entire sphere.

Meanwhile, we also notice that the expansion of G can also be limited to the first L terms, namely

$$G(\mathbf{r},\mathbf{r}') \propto \sum_{l=0}^{L}\sum_{m=-l}^{l} j_l(r')Y_l^m(\theta,\phi)Y_l^{m*}(\theta',\phi'), \tag{28}$$

due to the limited modes of J (the higher order modes in G cannot be triggered by the source).

2) Discretization and Conditioning: To this end, we consider the samples of fields on $\mathcal{M}_s$. When M measurements are taken at positions $\{(\theta_m,\phi_m)\}_{m=1,...,M}$ on $\mathcal{M}_s$, we can rewrite (27) in the matrix form:

$$\mathbf{e} = \mathbf{Y}\mathbf{c}, \tag{29}$$

where $\mathbf{e} = (E(\theta_1,\phi_1),...,E(\theta_M,\phi_M))$, $\mathbf{c} = (c_0^0, c_1^{-1},...,c_L^L)$ and $\mathbf{Y}_{ij} = j_l(r')Y_{l(j)}^{m(j)}(\theta_i,\phi_i)$, where $l^2+m=j$.

According to the linear relationship between the errors of current density and field measurement, denoted by ΔJ and ΔE, we have

$$\int_B G(\mathbf{r},\mathbf{r}')J_e(\mathbf{r}')d\mathbf{r}' = \Delta E(\mathbf{r}), \tag{30}$$

which implies the linear equation similar to (31):

$$\mathbf{e}_e = \mathbf{Y}\mathbf{c}_e, \tag{31}$$

where the subscript e indicates the error in the estimation or measurement. Therefore, we have

$$\frac{\|\mathbf{c}_e\|}{\|\mathbf{c}\|} \le \kappa(\mathbf{Y})\|\mathbf{e}_e\|, \tag{32}$$

where $\kappa(\mathbf{Y}) = \|\mathbf{Y}^\dagger\|\|\mathbf{Y}\|$ is the generalized condition number of $\mathbf{Y}$ and $\mathbf{Y}^\dagger$ is the generalized inverse. It is difficult to evaluate the condition number $\kappa(\mathbf{Y})$ analytically. Numerical results will be shown in Section VI.

3) Bounds via Cauchy-Schwartz Inequalities: An alternative approach to derive bounds for the sensing MSE is to leverage the forward and inverse Cauchy-Schwartz Inequalities. Consider $\mathbf{r}_* = \arg\max_{\mathbf{r}} \Delta E(\mathbf{r})$, namely the point at which the measurement error is the maximal. Then, we have

$$\int_B G(\mathbf{r}_*,\mathbf{r}')\Delta J(\mathbf{r}')d\mathbf{r}' = \Delta E(\mathbf{r}_*). \tag{33}$$

Using the Cauchy-Schwartz inequality, we have

$$\begin{aligned}&\int_B |G(\mathbf{r}_*,\mathbf{r}')|^2\mathbf{r}' \int_B |\Delta J(\mathbf{r}')|^2 d\mathbf{r}' \\ \ge\ & \left|\int_B G(\mathbf{r}_*,\mathbf{r}')\Delta J(\mathbf{r}')\right|^2 d\mathbf{r}' = |\Delta E(\mathbf{r}_*)|^2.\end{aligned} \tag{34}$$

Therefore, we can obtain a lower bound for the estimation error:

$$\int_B |\Delta J(\mathbf{r}')|^2 d\mathbf{r}' \ge \frac{|\Delta E(\mathbf{r}_*)|^2}{\int_B |G(\mathbf{r}_*,\mathbf{r}')|^2\mathbf{r}'}. \tag{35}$$

For obtaining an upper bound, we consider the following Pólya-Szegö's inequality, as an inverse of the Cauchy-Schwartz inequality.

Lemma 1. *Consider continuous functions a and b defined over a ball O. Define $m_1 = \min_x a(x)$, $m_2 = \min_x b(x)$, $M_1 = \max_x a(x)$, $M_2 = \max_x b(x)$. Then we have*

$$\frac{\int_O a^2(x)dx \int_O b^2(x)dx}{\left(\int_O a(x)b(x)dx\right)^2} \le \frac{1}{4}\left(\sqrt{\frac{M_1M_2}{m_1m_2}} + \sqrt{\frac{m_1m_2}{M_1M_2}}\right)^2. \tag{36}$$

Given (36), we obtain the upper bound for the sensing MSE:

$$\begin{aligned}\int_B |\Delta J(\mathbf{r}')|^2 d\mathbf{r}' \ &\le\ \frac{|\Delta E(\mathbf{r}_*)|^2}{\int_B |G(\mathbf{r}_*,\mathbf{r}')|^2\mathbf{r}'} \\ &\times\ \frac{1}{4}\left(\sqrt{\frac{M_1M_2}{m_1m_2}} + \sqrt{\frac{m_1m_2}{M_1M_2}}\right)^2,\end{aligned} \tag{37}$$

where the constants M_1, M_2, m_1 and m_2 are obtained from the EM field setup.

V. Trade-off Analysis

In this section, we summarize the performances of communications and sensing for different DoFs of EM fields, based on which we derive the trade-off between communications and sensing in JCS. For simplicity, we assume that all scatters are located within a ball B.

It is assumed that the bandwidth of the EM field due to the scatterers is W. Then, we have the following conclusions:

- Communications: The area of antenna array is given by $\frac{N_c}{\rho_c}$ for the communication receiver. Therefore, the DoF of samples at the communication receive antenna array is given by
$$DoF = \begin{cases} \frac{WN_c}{\rho_c}, \text{ if } W < \rho_c \\ N_c, \text{ if } W \ge \rho_c \end{cases}, \tag{38}$$
since the spatial bandwidth W represents the spatial density of DoF and N_c/ρ_c is the approximate area of the communication manifold $\mathcal{M}_c$.
- Sensing: When $W > \rho_s$, the measurement error at the sensing manifold will be large, thus making large errors in the field estimation of the scatterers. When $W < \rho_s$, summarizing (32) and (14), we have
$$\begin{aligned}\|\Delta J\|_2 \ &\le\ \frac{\omega\mu}{4\pi d}\left|\int_B |J(\mathbf{r}')|^2 d\mathbf{r}'\right|^{\frac{1}{2}} \frac{\exp\left(-\frac{2}{3}\sigma_{m,n}^{\frac{3}{2}}\right)}{2(\rho_s - W)} \\ &\times\ \max\kappa(\mathbf{Y}).\end{aligned} \tag{39}$$

Then, we denote by J_e the upper bound of $\|\Delta J\|_2$ in (39), which satisfies $J_e = \frac{C}{\rho_s - W}$, where C is the constant given by

$$C = \frac{\omega\mu}{8\pi d}\left|\int_B |J(\mathbf{r}')|^2 d\mathbf{r}'\right|^{\frac{1}{2}} \exp\left(-\frac{2}{3}\sigma_{m,n}^{\frac{3}{2}}\right)\max\kappa(\mathbf{Y}) \tag{40}$$

We define $D = \frac{DoF}{N_c}$, namely the communication DoF per receive antenna. Then, summarizing (38) and (39), we have

$$\begin{cases} \frac{C}{J_e} + D\rho_c = \rho_s, \text{ if } \rho_s, \rho_c \ge W \\ D = 1, \text{ if } \rho_c < W \\ J_e \to \infty, \text{ if } \rho_s < W \end{cases}. \tag{41}$$

When there are sufficiently many receive antennas, namely $\rho_c \ge W$, we observe that the trade-off between communications and sensing is given by $\frac{C}{J_e} + D\rho_c = \rho_s$; i.e., when the DoF of communications per antenna, namely D, increases, J_e (the upper bound of sensing error) also increases.

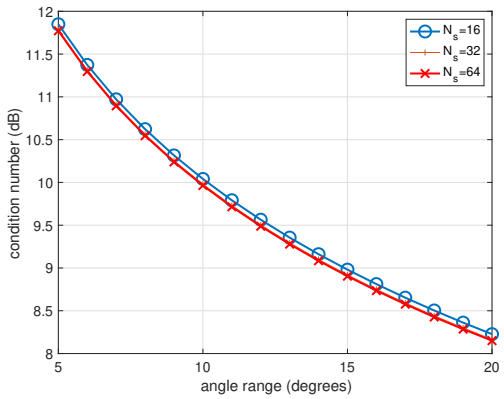

Fig. 5. Condition number $\kappa(\mathbf{Y})$.

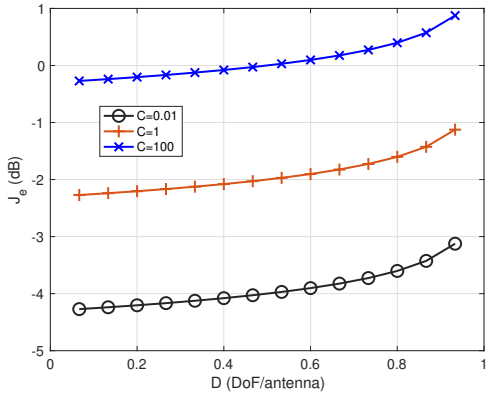

Fig. 6. Trade-off between communication DoF and sensing error.

VI. Numerical Results

In this section, we provide numerical results to illustrate the analytic conclusions in the above discussion.

A. Condition Number

In Fig. 5, we plotted the condition number $\kappa(\mathbf{Y})$ for different angle ranges of sensing manifold $\mathcal{M}_s$. We assume that $\mathcal{M}_s$ is an arc whose angle ranges from 5 to 20 degrees. Different numbers of antennas on $\mathcal{M}_s$, ranging from 16 to 64, are considered. The order of spherical harmonics is set to $L = 3$. Note that the condition number $\kappa(\mathbf{Y})$ is plotted in the dB scale. We observe that the condition numbers are large, which means that the sensing error of source currents over the scatterers is highly sensitive to the measurement error at the sensing manifold $\mathcal{M}_s$. Therefore, more regularization conditions are needed for the source current estimation.

B. Trade-off between Communications and Sensing

We plotted in Fig. 6 the trade-off curve between communications and sensing, based on (41). We assume that there are sufficiently dense antennas, namely $\rho_s, \rho_c \geq W$. It is further assumed that the antennas are placed with a half-wavelength spacing. By assuming the 60GHz band, the antenna spacing is 2.5mm. Different values of the constant C in (40) are tested. We observe the nonlinear increase of sensing MSE when the DoF of communications becomes large (e.g., greater than 0.8), which characterizes the conflict of interest between communications and sensing in JCS.

VII. Conclusions

In this paper, we have analyzed the DoF of the EM field of JCS. A higher DoF means more complex scatterers, thus improving the number of orthogonal communication channels, while increasing the difficulty of sensing. Therefore, a trade-off in the EM field DoF has been identified between communications and sensing, which has been characterized in an analytic manner. We have used numerical results to illustrate the corresponding trade-off. Our future research will be focused on the randomness incurred by stochastic scatterers.

References

[1] L. Han and K. Wu, "Joint wireless communication and radar sensing systems–state of the art and future prospects," *IET Microwaves, Antennas & Propagation*, vol. 7, no. 11, pp. 876–885, 2013.

[2] B. Paul, A. R. Chiriyath, and D. W. Bliss, "Survey of rf communications and sensing convergence research," *IEEE Access*, vol. 5, pp. 252–270, 2016.

[3] L. Zheng, M. Lops, Y. C. Eldar, and X. Wang, "Radar and communication co-existence: an overview," *arXiv preprint arXiv:1902.08676*, 2019.

[4] F. Liu, C. Masouros, A. Petropulu, H. Griffiths, and L. Hanzo, "Joint radar and communication design: Applications, state-of-the-art, and the road ahead," *IEEE Transactions on Communications*, 2020.

[5] D. Ma, N. Shlezinger, T. Huang, Y. Liu, and Y. C. Eldar, "Joint radar-communications strategies for autonomous vehicles," *IEEE Signal Processing Magazine*, vol. 37, no. 4, pp. 85–97, 2020.

[6] H. Li, "Inseparable waveform synthesis in joint communications and radar via spatial-frequency spectrum," in *Proc. of IEEE Global Communication Conference (Globecom)*, 2021.

[7] ——, "Conflict and trade-off of waveform uncertainty in joint communication and sensing systems," in *Submitted to IEEE International Conference on Communications (ICC)*, 2021.

[8] O. M. Bucci and G. Franceschetti, "On the spatial bandwidth of scattered fields," *IEEE Trans. on Antennas and Propagation*, vol. 35, no. 12, pp. 1445–1455, 1987.

[9] ——, "On the degrees of freedom of scattered fields," *IEEE Trans. on Antennas and Propagation*, vol. 37, no. 7, pp. 918–926, 1989.

[10] M. Kobayashi, H. Hamad, G. Kramer, and G. Caire, "Joint state sensing and communication over memoryless multiple access channels," *Proc. of IEEE International Symposium on Information Theory (ISIT)*, pp. 270–274, 2019.

[11] H. Li, "Dual function trade-off in joint communications and radar: An electromagnetic field analysis," in *Proc. of IEEE Global Communication Conference (Globecom)*, 2021.

[12] D. W. Bliss and H. Govindosamy, *Adaptive Wireless Communications: MIMO Channels and Networks*. Cambridge University Press, 2011.

[13] K. W. Forsythe, "Utilizing waveform features for adaptive beamforming and direction finding with narrow-band signals," *Lincoln Laboratory Journal*, vol. 10, no. 2, pp. 99–126, 1997.

[14] D. Gaglione, C. Clemente, C. V. Ilioudis, A. R. Persico, I. K. Proudler, J. J. Soraghan, and A. Farina, "Waveform design for communicating radar systems using fractional fourier transform," *Digital Signal Processing*, vol. 80, pp. 57–69, 2018.

[15] K. V. Mishra, M. B. Shankar, V. Koivunen, B. Ottersten, and S. A. Vorobyov, "Toward millimeter-wave joint radar communications: A signal processing perspective," *IEEE Signal Processing Magazine*, vol. 36, no. 5, pp. 100–114, 2019.

[16] M. D. Migliore, "On the role of the number of degrees of freedom of the field in mimo channels," *IEEE Trans. on Antennas and Propagation*, vol. 54, no. 2, pp. 620–628, 2006.

[17] ——, "On electromagnetics and information theory," *IEEE Trans. on Antennas and Propagation*, vol. 56, no. 10, pp. 3188–3200, 2008.

[18] M. Franceschetti, M. D. Migliore, and P. Minero, "The capacity of wireless networks: Information-theoretic and physical limits," *IEEE Trans. on Inform. Theory*, vol. 55, no. 8, pp. 3413–3424, 2009.

[19] N. G. de Brujin, *Asymptotic Methods in Analysis*. North-Holland Publishing CO., 1958.

[20] A. J. Devaney, *Mathematical Foundations of Imaging, Tomography and Wavefield Inversion*. Cambridge University Press, 2012.